Inorg. Chem. **2004**, *43*, 5681–5687

Structural and Functional Models of the Active Site of Zinc Phosphotriesterase

Håkan Carlsson,[†,‡] Matti Haukka,[§] and Ebbe Nordlander*[,†]

Inorganic Chemistry, Kemicentrum, Lund University, Box 124, SE-221 00 Lund, Sweden, and Department of Chemistry, University of Joensuu, Box 111, FIN-80101 Joensuu, Finland

Received December 18, 2003

In an attempt to prepare structural and functional models for the active site of the hydrolytic enzyme zinc phosphotriesterase, five new zinc complexes of the ligands 2,6-bis[*N*-(*N*-(carboxylmethyl)-*N*-((1-methylimidazol)-methyl)amine)methyl]-4-methylphenolate (BCIMP) and the corresponding asymmetric ligand 2-(*N*-isopropyl-*N*-((1-methylimidazolyl)methyl)aminomethyl)-6-(*N*-carboxylmethyl-*N*-((1-methylimidazolyl)methyl)aminomethyl)-4-methylphenol (ICIMP) have been synthesized, viz. Na[Zn_2(BCIMP)Ac_2] (**1**), [Zn_2(BCIMP)(Ph_2Ac)] (**2**), [Zn_2(ICIMP)Ac_2] (**3**), [Zn_4(ICIMP)$_2$(Me_3Ac)$_2$][ClO_4]$_2$ (**4**), and [Zn_4(ICIMP)$_2$(Ph_2Ac)$_2$][ClO_4]$_2$ (**5**). The X-ray structure of complex **5** has been determined and reveals that the complex is a dimer of dimers in the solid state, which in solution dissociates to potent structural models. Studies using NMR show that only one carboxylate coligand bridges the dizinc units in the case of diphenyl acetate and pivalate, while the steric bulk of acetate is sufficiently small to permit the coordination of two acetates/dizinc unit. Functional studies involving the hydrolysis/transesterification of 2-hydroxypropyl *p*-nitrophenyl phosphate (HPNP) show that the complex with ICIMP (compound **5**) has a significantly higher rate of catalysis than the BCIMP complex (compound **2**). This is attributed to the vacant/labile coordination site that is available in the ICIMP complex but not the BCIMP complex.

Introduction

Zinc ions are a vital part of all biological systems, and among the trace metals, zinc is second only to iron in abundance in the human organism. In living systems, zinc has structural properties, e.g. in the zinc fingers,[1] as well as catalytic functions,[2] and it has been found in the active sites of hydrolytic enzymes in over 200 cases.[3] The ability to assist in Lewis activation, nucleophile generation, and leaving group stabilization has made zinc, and especially dinuclear zinc sites, ideal for catalysis of hydrolytic reactions.[4−6] Several hydrolytic dizinc enzymes are known; β-lactamases,[7] aminopeptidases,[8] and zinc phosphotriesterase are a few examples. The latter is especially interesting due to its ability to hydrolyze organophosphates, and its reactivity toward warfare reagents such as sarin and VX has made it a potential choice for bioremediation.[9] The enzyme is normally found and isolated from earth-dwelling bacteria, such as *Pseudomonas diminuta*, from which X-ray structures also are available.[9,10] The active site (Figure 1) shows many similarities to the active site of the nickel enzyme urease.[11] Each of the two zinc ions is coordinated by two histidine residues from the protein backbone. A carbamylated lysine residue and a hydroxide group are bridging the ions, and an aspartate residue is asymmetrically bound to one of the zinc centers. The distance between the zinc ions is about 3.4 Å, which is similar to urease (3.5 Å).[11] Several mechanisms are possible for phosphoesterases.[12] The origin of the attacking oxygen

* Author to whom correspondence should be addressed. E-mail: Ebbe.Nordlander@inorg.lu.se.
† Lund University.
‡ Current affiliation: Azusa Pacific University, Azusa, CA.
§ University of Joensuu.

(1) Matthews, J. M.; Sunde, M. *IUBMB Life* **2002**, *54*, 351.
(2) Kaim, W.; Schwederski, B. *Bioinorganic Chemistry: Inorganic Elements in the Chemistry of Life*; Wiley: New York, 1994; p 242.
(3) Gultneh, Y.; Khan, A. R.; Blaise, D.; Chaudhry, S.; Ahvazi, B.; Marvey, B. B.; Butcher, R. J. *J. Inorg. Biochem.* **1999**, *75*, 7.
(4) Erxleben, A.; Hermann, J. *J. Chem. Soc., Dalton Trans.* **2000**, 569.
(5) Bashkin, J. K. *Curr. Opin. Chem. Biol.* **1999**, *3*, 752.
(6) Wilcox, D. E. *Chem. Rev.* **1996**, *96*, 2435.
(7) Wang, Z.; Fast, W.; Valentine, A. M.; Benkovic, S. J. *Curr. Opin. Chem. Biol.* **1999**, *3*, 614.
(8) Sträter, N.; Lipscomb, W. N. *Biochemistry* **1995**, *34*, 14792.
(9) Benning, M. M.; Shim, H.; Raushel, F. M.; Holden, H. M. *Biochemistry* **2001**, *40*, 2712.
(10) Vanhooke, J. L.; Benning, M. M.; Raushel, F. M.; Holden, H. M. *Biochemistry* **1996**, *35*, 6020.
(11) (a) Jabri, E.; Carr, M. B.; Hausinger, R. P.; Karplus, P. A. *Science* **1995**, *268*, 998. (b) Benini, S.; Rypniewski, W. R.; Wilson, K. S.; Miletti, S.; Ciurli, S.; Mangani, S. *Structure* **1999**, *7*, 205.
(12) Kimura, E. *Curr. Opin. Chem. Biol.* **2000**, *4*, 207.

10.1021/ic0354522 CCC: $27.50
Published on Web 08/13/2004

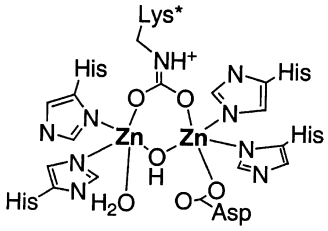

Figure 1. Schematic depiction of the structure of the active site of *Pseudomonas diminuta*.[10]

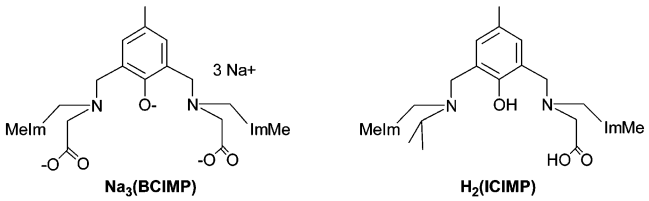

Figure 2. Schematic structure of BCIMP (2,6-bis[*N*-(*N*-(carboxylmethyl)-*N*-((1-methylimidazol)methyl)amine)methyl]-4-methylphenolate) and ICIMP (2-(*N*-isopropyl-*N*-((1-methylimidazolyl)methyl)aminomethyl)-6-(*N*-carboxylmethyl-*N*-((1-methylimidazolyl)methyl)aminomethyl)-4-methylphenol)).

atom is the main controversy. The bridging hydroxide, a terminally bound hydroxo group, or an activated free water molecule have been mentioned as possibilities.

With the goal to synthesize a structural/functional model for zinc phosphotriesterase and to study its reactivity, we have prepared dizinc complexes of the ligands BCIMP and ICIMP[13] (Figure 2) and attempted to study the importance of an asymmetric ligand environment that introduces a vacant (or weakly coordinated) coordination site at one of the zinc atoms. Thus, the reactivity of a symmetric Zn_2BCIMP complex with coordinatively saturated zinc ions has been compared to a corresponding asymmetric Zn_2ICIMP complex with an available coordination site. The crystal structure of one of the complexes is presented, and functional studies modeling the hydrolysis of both RNA and DNA are discussed.

Results and Discussion

Dinuclear complexes with alkoxide or phenoxide bridges are frequently used in modeling of enzyme active sites,[14−19] but it is not until recently that ligands with both carboxylate and imidazole ligands have been made available.[13] In an attempt to prepare suitable models for zinc phosphotriesterase, five new zinc complexes were synthesized. Two are based on the symmetric ligand BCIMP (**1**, **2**), while three are based on the asymmetric ligand ICIMP (**3**−**5**). To our knowledge, these are the first dinuclear zinc complexes in which both imidazole and carboxylate ligands together constitute a suitable ligand environment for a model for the histidine- and aspartate-ligated active site of zinc phosphotriesterase.

Synthesis of the Symmetric Complexes $[Zn_2(BCIMP)Ac_2]^-$ (1) and $[Zn_2(BCIMP)(Ph_2Ac)]$ (2). Zinc perchlorate was used as a source of zinc in all syntheses. **Caution!** *Perchlorate salts of metal complexes with organic ligands are potentially explosive and should be handled accordingly.* When zinc perchlorate was reacted with Na_3BCIMP and sodium acetate or diphenyl acetate in methanol solutions, white solids of the complexes $[Zn_2(BCIMP)Ac_2]^-$ **(1)** and $[Zn_2(BCIMP)(Ph_2Ac)]$ **(2)**, respectively, were generated upon careful addition of diethyl ether. The compounds have been analyzed by ^{1}H NMR, IR, and MS. Minor changes in shifts (relative to the uncomplexed ligand) are seen for all BCIMP resonances in the ^{1}H NMR spectra of **1** and **2**. As expected, downfield shifts compared to free ligand are found for moieties in close proximity to the metals, consistent with electron donation to the zinc ions.[20] The changes are significantly larger in the case of groups close to the metal ions (methylenes, 3.59 to 3.75−3.80 ppm) than for groups further away (e.g. phenol methyl, 2.17 to 2.14 ppm). Integration supports the stoichiometric assignments with two acetate ligands/two zinc ions in **1** and one diphenyl acetate/two zinc ions in **2**. In **1**, the integral for the acetate signal at 2.01 is twice that of the phenol methyl group at 2.17 and the same as the aromatic region (6 H, imidazole resonances included). In the case of **2**, a similar situation is seen where the downfield aromatic group originating from the phenyl groups in diphenyl acetate integrates to 10 H, while the phenol methyl group and the rest of the aromatic signals come to 3 H and 6 H, respectively. In addition, the diphenyl acetate methyline hydrogen integrates to 1 H. To ensure solubility and to avoid solvent/solute overlap of the NMR signals, **1** and **2** were run in both CD_3CN and CD_3OD.

The differences in IR between the symmetric and asymmetric stretches of carboxylate groups can be used to predict their coordination modes in complexes.[21] On the basis of IR data reported for dinuclear zinc complexes in several studies,[18,22,23] we note that that an asymmetric stretch at higher wavenumbers than 1600 cm^{-1} in the zinc complexes usually indicates a carboxylate ligand coordinated in a unidentate fashion. If the stretch falls below 1600 cm^{-1}, it is more likely to originate from a bridging carboxylate. In the cases of complex **1** and **2**, there are two different asymmetric stretches, one around 1625 cm^{-1} and one around 1590 cm^{-1}, consistent with unidentate and terminally coordinated, as well as bridging, coordination modes for the carboxylates in the complexes. Comparison of the symmetric and asymmetric IR stretches gives the same results, but the

(13) Carlsson, H.; Haukka, M.; Nordlander, E. *Inorg. Chem.* **2002**, *41*, 4981.
(14) Adams, H.; Bradshaw, D.; Fenton, D. E. *Supramol. Chem.* **2001**, *13*, 513.
(15) Albedyhl, S.; Schnieders, D.; Jancso, A.; Gajda, T.; Krebs, B. *Eur. J. Inorg. Chem.* **2002**, 1400.
(16) Abe, K.-J.; Izumi, J.; Ohba, M.; Yokoyama, T.; Okawa, H. *Bull. Chem. Soc. Jpn.* **2001**, *74*, 85.
(17) Adams, H.; Bradshaw, D.; Fenton, D. E. *Inorg. Chim. Acta* **2002**, *332*, 195.
(18) Uhlenbrock, S.; Krebs, B. *Angew. Chem.* **1992**, *104*, 1631.
(19) Lanznaster, M.; Neves, A.; Bortoluzzi, A. J.; Szpoganicz, B.; Schwingel, E. *Inorg. Chem.* **2002**, *41*, 5641.
(20) Carlsson, H.; Haukka, M.; Bousseksou, A.; Latour, J.-M.; Nordlander, E. Submitted for publication in *Inorg. Chem.*
(21) Deacon, G. B.; Phillips, R. J. *Coord. Chem. Rev.* **1980**, *33*, 227.
(22) Chen, X.-M.; Tong, Y.-X.; Mak, T. C. W. *Inorg. Chem.* **1994**, *33*, 4586.
(23) Ye, B.-H.; Li, X.-Y.; Williams, I. D.; Chen, X.-M. *Inorg. Chem.* **2002**, *41*, 6426.

symmetric stretches are harder to discern and therefore more prone to errors. The observed IR spectra are in agreement with structures where the ligand (BCIMP) carboxylate is terminal and the coligand(s) is/are bridging. For both complexes, the mass spectra indicate the presence of $Na[Zn_2(BCIMP)(A^-)]$ ($A^- = Ac$, Ph_2Ac) and $Zn_2(BCIMP)$ fragments. Verification of the exact masses has been made by high-resolution mass spectrometry (cf. Experimental Section).

The molecular structure of the dinickel complex $[Ni_2(BCIMP)Ac_2]^-$ has been established by X-ray crystallography.[20] As mentioned above, the mass spectrum of complex **1** is consistent with the formulation $[Zn_2(BCIMP)Ac_2]^-$ and the similar ionic radii of Ni(II) and Zn(II) (0.69 vs 0.74 Å) suggest that the dizinc complex is isostructural with the structurally characterized dinickel complex; i.e., each metal ion is hexacoordinate, with the donor atoms provided by BCIMP and two bridging acetates. The ligand-to-coligand 1:2 stoichiometry suggested by the NMR studies has been observed for dinickel complexes of BCIMP with acetate or diphenylacetate ligands.[20,24]

Synthesis and Characterization of Asymmetric Complexes of ICIMP. The formation of complexes of the asymmetric ligand ICIMP could be followed visually. As the zinc solution was added to a yellow solution of ICIMP and a suitable carboxylate salt, the yellow color quickly faded to yield a nearly colorless solution. The product of the reaction with sodium acetate, **3**, was found to easily dissolve in water, while products **4** and **5**, containing pivalic and diphenyl acetic acid, respectively, were found to be sufficiently nonpolar to precipitate from the ethanolic reaction mixture. Compounds **3**−**5** were characterized by NMR, IR, and UV/vis spectroscopy, mass spectrometry, and, in the case of **4** and **5**, elemental analysis. The features that were observed for the NMR spectra of the BCIMP complexes were also detected in the ICIMP complexes. Thus, the integrations of the aromatic region show that one pivalate and one diphenyl acetate are coordinated in complexes **4** and **5**, respectively. Similar changes in shift for the hydrogen atoms close to the coordination sites are also observed (cf. Experimental Section).

The carboxylate stretches are found at 1605 and 1561 cm^{-1} in complex **4** and 1607 cm^{-1} and 1592 cm^{-1} for complex **5**, indicating the presence of bridging and terminally coordinated carboxylate groups in both complexes. The relatively low frequency of the stretch assigned to the terminal carboxylate suggests the possibility of a "pseudobridging" coordination mode. This is consistent with a tetranuclear structure, where the terminal ligand carboxylate acts as the bridging identity to the neighboring tetramer. Evidence for a tetrameric structure in complex **4** also comes from the mass spectrum, and the crystal structure of complex **5** (vide infra) shows that this complex is tetranuclear in the solid state.

The observed mass spectrum of **3** indicates that this complex is dinuclear with the formulation $[Zn_2(ICIMP)Ac_2]$, which is expected to be isostructural with $[Zn_2(BCIMP)Ac_2]^-$ (**1**) but with one carboxylmethyl ligand donor arm missing. Assuming *pseudo*octahedral coordination geometries around each Zn ion, there is a coordination site on one metal that may be vacant or filled by a loosely coordinated solvent molecule. The markedly different solubility properties of **4** and **5** with respect to **3** are demonstrated by the immediate precipitation of **4** from water upon the addition of pivalic acid. The reason for the different solubilities is seen in the mass spectrum of complex **4** and the solid-state structure of **5**. Due to the steric hindrance of the bulkier carboxylates, only one carboxylate can fit into the dinuclear complex and the FAB mass spectra of **4** and **5** are consistent with the formulations $[Zn_2(ICIMP)(carboxylate)]$ and expected structures corresponding to that of complex **2** but involving one five-coordinate and one four-coordinate Zn ion (or solvated forms of such a basic structure). However, in the case of **4**, an additional peak envelope corresponding to a tetranuclear ion $[Zn_4(ICIMP)_2(Me_3Ac)_2ClO_4]$ could be detected. This is consistent with the dimerization of two of the corresponding dinuclear complexes via one of the terminal ICIMP carboxylates as has been observed in the case of the tetranuclear nickel complexes $[Ni_4(ICIMP)_2(Ph_2Ac)_2(DMF)_2][ClO_4]_2 \cdot 2.5DMF$ and $[Ni_4(ICIMP)_2(Ph_2Ac)_2(urea)(H_2O)][ClO_4]_2 \cdot 0.5EtOH \cdot H_2O$.[13]

Table 1. Crystallographic Data for Compound **5**

empirical formula	$C_{76}H_{86}Cl_2N_{12}O_{18}Zn_4$
fw	1787.95
temp, K	150(2)
wavelength, Å	0.710 73
cryst syst	monoclinic
space group	$P2_1/n$
a, Å	12.171 30(10)
b, Å	13.5027(2)
c, Å	23.9281(5)
α, deg	90
β, deg	97.4863(5)
γ, deg	90
V, Å^3	3898.95(10)
Z	2
ρ_{calc}, g/cm^3	1.523
μ(Mo Kα), mm^{-1}	1.362
$R_1{}^a$ ($I \geq 2\sigma(I)$)	0.0440
$wR_2{}^b$ ($I \geq 2\sigma(I)$)	0.0985

^{a} $R_1 = \sum||F_o| - |F_c||/\sum|F_o|$. ^{b} $wR_2 = [\sum[w(F_o^2 - F_c^2)^2]/\sum[w(F_o^2)^2]]^{1/2}$.

For complex **5**, crystals of X-ray quality could be grown and the crystal structure was determined to identify the structure and nuclearity of the complex. Crystallographic data are summarized in Table 1. As is shown in Figure 3, the crystal structure reveals a tetranuclear complex. The asymmetric unit of the complex contains one dimer and the unit cell contains four asymmetric units or two complexes. The Zn−Zn distance is 3.459(1) Å, which is close to the value found in the enzyme crystal structure (3.4 Å).[25] The metal-to-ligand distances are close to those found in other similar systems.[4,16,17] The ligand orientation around the metal centers is distorted trigonal bipyramidal; the distortion may be attributed to the strain/rigidity of the ligand backbone. The Zn−

(24) In the case of $[Ni_2(BCIMP)(Ph_2Ac)_2]^-$, the mass spectrum reveals peaks attributable to $[Ni_2(BCIMP)(Ph_2Ac)_2]^-$ (70% relative intensity) and $[Ni_2(BCIMP)(Ph_2Ac)]$ (100% relative intensity).

(25) Benning, M. M.; Shim, H.; Raushel, F. M.; Holden, H. M. *Biochemistry* **2001**, *40*, 2712.

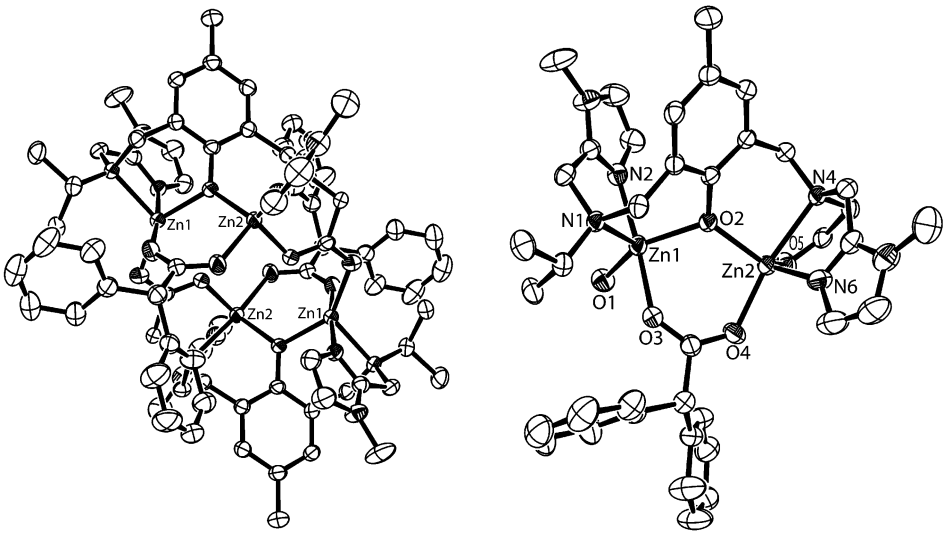

Figure 3. ORTEP representations of the molecular structure of the complete compound **5** and the asymmetric entity, respectively. Some relevant average bond distances and bond angles for the two asymmetric units in compound **5**: Zn---Zn 3.459(1) Å, Zn−N(amine) 2.233 Å, Zn−N(imidazole) 2.081 Å, Zn−O(term. carbox) 2.014(0) Å, Zn−O(bridg phenoxide) 2.032 Å; Zn−O−Zn 120.09(0)°, N(amine)−Zn−N(imidazole) 79.06°.

N(amine) distances are for the same reason longer than expected for a regular Zn−N bond (2.23 Å in **5** vs 2.05 Å for some selected Zn−unidentate ligand distances[26−29]). This is also the case for the carboxylate ligand (2.03 Å vs 1.94 Å[30−32]), while the imidazole ligand is close to normal (2.05 Å vs 2.06 Å).[33−35] The strain in the carboxylate ligand distance seems to arise from its secondary interaction with the neighboring dimer.

In contrast to the corresponding nickel complexes[13] (vide supra), the tetramer is completely symmetric. However, the dimeric forces seem to be weak and the Zn_2 units appear to be easily separable since the tetramer cannot be detected in the mass spectrum. Dissociation is probably taking place when the complex is dissolved in a coordinating solvent. It is probable that the same phenomenon is observed for complex **4**.

Hydrolysis of 2-Hydroxypropyl *p*-Nitrophenyl Phosphate (HPNP). Since it is still not certain whether zinc phosphotriesterase does have any natural phosphotriester substrate[36] and since phospotriesters in general are very toxic, the transesterification of HPNP was used as an assay to estimate the catalytic activity of the complexes toward phosphoesters and RNA.[36] The conditions were chosen to allow comparisons with other published systems.[37] Since no tetramers could be detected in the dissolved complex (by mass spectrometry), compound **5** ("$[Zn_2(ICIMP)(Ph_2Ac)]$") was chosen as the best structural model for Zn phosphotriesterase. Initial rates were determined for the hydrolysis at pH values between 7 and 9. In Figure 4, the data can be compared to the corresponding nickel complex and the uncatalyzed rate, all in Tris buffer. At physiological pH, the rate was found to be significantly faster for **5** than the corresponding nickel complex, but even at the higher pH, the rate for the zinc complex is about five times faster than the nickel complex. This may be attributed to the stronger Lewis acidity of zinc; i.e., the pK_a of water is lowered more by coordination to zinc than to nickel and this might be one of the reasons for the fact that the optimum pH for urease (pH 8.0) is higher than for zinc phosphotriesterase (from pH 6.5).[36] (Other factors, such as the optimum pH for the hydrolysis of the carbamate product of urease, may contribute to the optimum pH of this enzyme.)

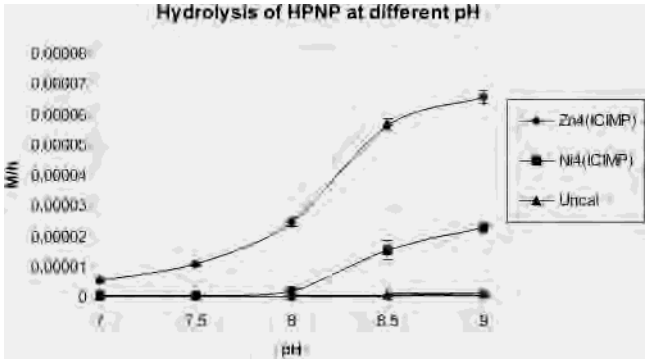

Figure 4. Dependence on the initial rates of hydrolysis of HPNP at different pH values for Zn_4(ICIMP) and Ni_4(ICIMP) catalyzed and uncatalyzed reactions.

To study the importance of the site asymmetry and the availability of coordination sites on the zinc ions, the

(26) Ma, Y.; Lai, T.; Wu, Y. *Adv. Mater.* **2000**, *12*, 433.
(27) Mutikainen, I. *Inorg. Chim. Acta* **1987**, *136*, 155.
(28) Ruth, M. B.; Foxman, B. M. *Mol. Cryst. Liq. Cryst. Sci. Technol., Sect. A* **2001**, *356*, 61.
(29) Guggenberger, L. J. *Inorg. Chem.* **1969**, *8*, 2771.
(30) Wang, R.; Hong, M.; Liang, Y.; Cao, R. *Acta Crystallogr., Sect. E* **2001**, *E57*, m277.
(31) Moriuchi, T.; Nishiyama, M.; Hirao, T. *Eur. J. Inorg. Chem.* **2002**, 447.
(32) Demirhan, F.; Gun, J.; Lev, O.; Modestov, A.; Poli, R.; Richard, P. *J. Chem. Soc., Dalton Trans.* **2002**, 2109.
(33) Korp, J. D.; Bernal, I.; Merrill, C. L.; Wilson, L. J. *J. Chem. Soc., Dalton Trans.* **1981**, 1951.
(34) Kojima, Y.; Hirotsu, K.; Yamashita, T.; Miwa, T. *Bull. Chem. Soc. Jpn.* **1985**, *58*, 1894.
(35) Sandmark, C.; Brändén, C. I. *Acta Chem. Scand.* **1967**, *21*, 993.
(36) Raushel, F. M.; Holden, H. M. *Adv. Enzymol. Relat. Areas Mol. Biol.* **2000**, *74*, 51.
(37) Albedyhl, S.; Averbuch-Pouchot, M. T.; Belle, C.; Krebs, B.; Pierre, J. L.; Saint-Aman, E.; Torelli, S. *Eur. J. Inorg. Chem.* **2001**, 1457.

Table 2. Initial Rates of Hydrolysis of HPNP by Compounds **2**, **3**, and **5** Compared to Published Catalysts[20,37]

catalyst	init rate (10^{-5} M/h)	rate ratio vs uncatal
2	0.10	7
3	2.32	167
5	2.45	176
zinc acetate	0.94	68
$[Ni_4(ICIMP)_2]^{4+}$ in Tris buffer	0.19	13
$[ZnFe(BPMOP)]^{4+}$	2.1	112
$[ZnFe(BPMP)]^{4+}$	1.0	54
$[Fe_2(BPMOP)]^{4+}$	3.0	11
$[Fe_2(BPMOP)]^{4+}$	0.059	3

hydrolytic activity of $[Zn_2(BCIMP)(Ph_2Ac)]$ **2** was studied at pH 8.0 and compared to the results obtained with complex **5**. In Table 2, the two systems can be compared to each other and to previously published systems. As may be seen, the rate is much slower for the symmetric complex **2** and comparable to the activity of free zinc acetate. The catalytic function of the zinc complex, and most likely the initial association of the product to the active site, appear to benefit from one more open coordination site on one zinc ion. It may be noted that zinc acetate has a catalytic activity that supersedes compound **2**. It is, however, clear that the ICIMP ligand in complex **5** has a positive effect on the activity (cf. Conclusions).

DNA Hydrolysis. The ability of one of the above-mentioned zinc complexes to hydrolyze plasmid DNA (pUC18) was investigated. Complex **3** was chosen as it is assumed to possess a vacant coordination site and is soluble in water. To verify the general hydrolytic ability of **3**, it was assayed by the HPNP hydrolysis reaction, and as can be seen in Table 2, it is a potent hydrolytic catalyst comparable to complex **5**. The similar catalytic activities of **3** and **5** suggest that the most important criterion for catalytic activity is one nominally vacant coordination site at which water can bind and be deprotonated and that the total number of such vacant sites is of lesser importance for the ability of the complex to catalyze the DNA hydrolyses studied here. The DNA electrophoresis gel can be seen in Figure 5. The different bands have been labeled. From the leftmost lanes, 1 and 2, which contain unhydrolyzed DNA, the amount of supercoiling can be estimated to about 75%. An effect of the incubation can be seen, lowering the supercoiling to around 50%. In lanes 4 and 5, the Fenton reagent has completely digested the DNA. The experiment has been repeated three times with the same result. In lanes 6 and 7, complex **3** has been allowed to react with the DNA. No major change can be seen vs the uncatalyzed, unincubated DNA. The supercoiled-to-circular ratio is about 50%. In contrast, in lane 8, where DNA has been reacted with zinc acetate, an effect is seen. The supercoiled level has been lowered to between 5 and 10%, and a weak band corresponding to linear DNA can be seen. The experiment with complex **3** at pH 10 shows results similar to those of the experiment at physiological pH.

The experiment shows that complex **3** has a very low ability to catalyze hydrolysis of DNA, much lower than zinc acetate. This is opposite to what was observed in the case of the HPNP hydrolysis (vide supra). There are two possible

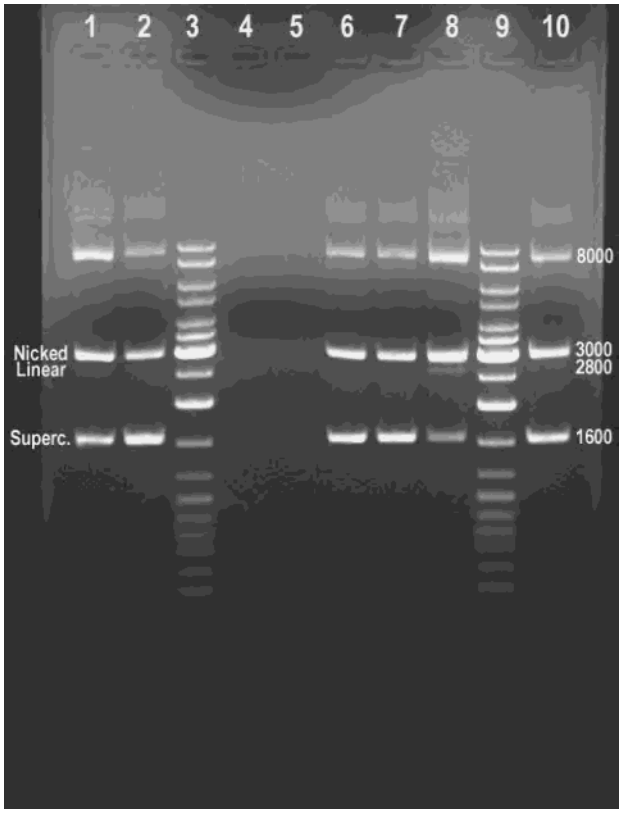

Figure 5. Agarose gel (1.0%) showing the hydrolysis of plasmid DNA (pUC18) using different catalysts and pH: lane 1, DNA at pH 7, no catalyst, incubated at 37 °C overnight; lane 2, as lane 1 not incubated; lanes 3 and 9, DNA ladder (Fermentas Generuler); lanes 4 and 5, DNA incubated with Fenton reagent, prepared from iron(II) sulfate (40 μM) and hydrogen peroxide (500 μM), overnight; lanes 6 and 7, DNA incubated with compound **3** at pH 7 and incubated overnight at 37 °C; lane 8, DNA incubated with zinc acetate at pH 7 overnight; lane 10, DNA incubated with compound **3** at pH 10 and incubated overnight at 37 °C.

explanations for these observations. The mechanism might depend on an easily accessible nucleophile, which is present through the internal hydroxide available in HPNP. On the other hand, this would make it hard to explain the comparatively low effect of free zinc ions in the HPNP hydrolysis and that the enzyme readily reacts with molecules without such a group. Another explanation is that the steric hindrance of the supercoiled DNA molecule makes it comparatively harder for a relatively large metal complex to approach the DNA and catalyze hydrolysis. Hydrated zinc ions are much smaller and have easier access to the coiled structure and the phosphoester bonds than the bulkier model complex (**3**). Such a steric effect is not seen for the smaller HPNP molecule and for the small substrates of the enzyme.

Conclusions

With the goal to make new structural and functional models for zinc phosphotriesterase, five new dinuclear zinc complexes were synthesized. Two were based on the symmetric ligand BCIMP, and three were based on the asymmetric ligand ICIMP. In the synthesis of the BCIMP complexes, we discovered that the addition of diphenyl acetate as a coligand prevented the association of a second carboxylate ion. The corresponding behavior was seen in the

complexes formed from the ICIMP ligand. However, the ICIMP/diphenyl acetate complex possesses a sufficiently open coordination sphere to allow coordination of a neighboring dizinc complex to create tetramers. Mass spectrometry indicates that these tetramers (dimers of dimers) dissociate in solution. When the functional behavior is compared for the two diphenyl acetate models, a clear difference in (catalytic) rates is noted. The ICIMP complex, which has one open (or weakly ligated) coordination site, can catalyze the hydrolysis of HPNP approximately five times faster than the BCIMP complex. This underscores the importance of the open coordination site in the hydrolytic mechanism. It is also apparent that the activity can be reasonably high even if the bridging hydroxide found in the active site of zinc phosphotriesterase is represented by a phenol moiety which cannot act as a nucleophile in the hydrolytic reaction. This observation suggests that the hydrolytic oxygen donor originates from, or is activated by,[38] a terminally bound hydroxo group although the present results obtained with HPNP as a substrate admittedly do not provide conclusive evidence that a metal-coordinated hydroxide moiety is the active nucleophile in the hydrolytic reaction. The mechanisms that are usually considered for metal catalyzed transesterification of HPNP[38,39] involve either (i) deprotonation of the HPNP alcohol moiety by a metal-bound hydroxide or (ii) coordination and deprotonation of the HPNP alcohol moiety to the metal and subsequent intramolecular nucleophilic attack. In principle, a metal-bound hydroxide may also deprotonate a free water molecule to generate a free hydroxide ion that instigates substrate transesterification.

The model complexes are poor catalysts for the hydrolysis of (supercoiled) DNA. This is proposed to be due to steric hindrance that prevents the model complex to access the phosphoester backbone of supercoiled DNA.

Experimental Section

Materials. The ligands BCIMP, 2,6-bis[*N*-(*N*-(carboxylmethyl)-*N*-((1-methylimidazol)methyl)amine)methyl]-4-methylphenolate, and ICIMP, 2-(*N*-isopropyl-*N*-((1-methylimidazolyl)methyl)aminomethyl)-6-(*N*-carboxylmethyl-*N*-((1-methylimidazolyl)methyl)aminomethyl)-4-methylphenol, were prepared according to previously published methods.[20] The other reactants were purchased commercially and used as received.

Physical Measurements. The electronic spectra and kinetic measurements were recorded on a Varian 300 Bio UV/vis spectrophotometer. Infrared spectra were collected on solid KBr disks on a Biorad FTS 6000 FT-IR spectrometer. Several samples indicated the presence of residual water from solvents; water in the KBr medium was ruled out in control experiments. NMR data was recorded on a Varian Unity 300 MHz spectrometer. Fast atom bombardment (FAB+) and high-resolution mass spectra were measured on a JEOL SX-102 instrument.

Synthesis of Complexes. Na[Zn_2(BCIMP)Ac_2] (1). Zinc perchlorate hexahydrate (93 mg, 0.25 mmol) was dissolved in methanol (2 mL). Sodium acetate (21 mg, 0.25 mmol) and Na_3BCIMP (67 mg, 0.125 mmol) were dissolved separately in methanol (3 mL). The ligand solution was added slowly to the zinc solution. After 15 min of stirring, diethyl ether was added dropwise until a white solid precipitated. The solid was filtered out, washed in methanol, and dried to yield 88 mg (95%) of product (**1**). FAB-MS [*m*/*z* (rel intensity, %)]: 679 (Na[Zn_2BCIMP(Ac)], 100), 597 (Zn_2BCIMP, 30). HRMS: 677.0659 (calcd exact mass Na[Zn_2BCIMP(Ac)], 677.0657). IR (KBr disk; cm^{-1}): 3556 (s), 3436 (s), 3138 (m), 2926 (m), 2863 (w), 2362 (w), 2337 (w), 2025 (w), 1622 (s), 1587 (s), 1510 (m), 1477 (m), 1420(s), 1397 (s), 1325 (m), 1285 (w), 1270 (w), 1103 (s), 1018 (w), 958 (w), 928 (w), 867 (w), 800 (m), 750 (m), 675 (m), 623 (s), 495 (m), 431 (w). UV/vis (MeCN; nm): 354 (br, sh), 291 (s). NMR (MeCN-d_3): δ 2.08 (s), 2.14 (s), 3.31 (s), 3.45 (m), 3.66 (m), 4.02 (d), 6.79 (br). NMR (CD_3OD): δ 2.01 (s), 2.17 (s), 3.42 (s), 3.57 (s), 3.75 (m), 4.01 (m), 6.88 (m).

[Zn_2(BCIMP)(Ph_2Ac)] (2). Zinc perchlorate hexahydrate (93 mg, 0.25 mmol) was dissolved in methanol (2 mL). Diphenyl acetic acid (53 mg, 0.25 mmol), sodium methoxide (14 mg, 0.25 mmol), and Na_3BCIMP (67 mg, 0.125 mmol) were dissolved in methanol (3 mL) in a second vial and mixed with the zinc perchlorate solution. After 15 min of stirring, diethyl ether was added dropwise until a white solid precipitated. The solid was filtered out, washed in methanol, and dried to yield 91 mg (90%) of complex (**2**). FAB-MS [*m*/*z* (rel intensity, %)]: 833 (Na[Zn_2BCIMP(Ph_2Ac)], 100), 597 (Zn_2BCIMP, 47). HRMS: 833.1299 (calcd exact mass Na-[Zn_2BCIMP(Ph_2Ac)], 829.1283). IR (KBr disk; cm^{-1}): 3553−3452 (s, br), 3132 (m), 3026 (w), 2923 (m), 2860 (m), 2860 (m), 2027 (w), 1629 (s), 1598 (s), 1510 (m), 1476 (s), 1451 (w), 1389 (s), 1286 (w), 1268 (w), 1165 (w), 1102 (s, br), 958 (m), 928 (w), 867 (m), 798 (w), 746 (m), 705 (w), 623 (m), 493 (w), 435 (w). UV/vis (MeCN; nm): 358 (sh, br), 292 (s). NMR (MeCN-d_3): 2.11 (s), 3.31 (m), 3.39 (m), 3.65 (m), 3.95 (m), 5.05 (br), 6.79 (br), 7.24 (br). NMR (CD_3OD): δ 2.14 (s), 3.51 (m), 3.69 (m), 3.80 (m), 5.05 (s), 6.80 (m), 7.27 (m).

[Zn_2(ICIMP)Ac_2] (3). Zinc perchlorate hexahydrate (112 mg, 0.30 mmol) was dissolved in water (3 mL). Sodium acetate (25 mg, 0.30 mmol) and H_2ICIMP (68 mg, 0.15 mmol) were separately dissolved in water (3 mL). The ligand solution was added to the zinc solution, and the resulting product solution was analyzed. FAB-MS [*m*/*z* (rel intensity, %)]: 641 (Zn_2ICIMP(Ac)], 100). HRMS: 639.1252 (calcd exact mass Na[Zn_2BCIMP(Ac)], 639.1252). IR (evap in KBr disk; cm^{-1}): 3416 (s, br), 2980 (w), 2930 (w), 2028 (w), 1607 (s), 1519 (w), 1481 (m), 1411 (m), 1334 (w), 1147 (s), 1090 (s), 952 (m), 940 (w), 873 (m), 804 (m), 770 (w), 758 (w), 661 (m), 637 (s), 626 (s), 501 (w). UV/vis (MeCN; nm): 295 (s). NMR (MeCN-d_3): δ 1.08 (m), 1.21 (s, br), 2.15 (s), 3.20 (s), 3.56 (m), 3.70 (m), 3.83 (m), 4.02 (s, br), 6.68 (m, br), 6.87 (m, br), 7.01 (s).

[Zn_4(ICIMP)$_2$(Me_3Ac)$_2$][ClO_4]$_2$ (4). Zinc perchlorate hexahydrate (112 mg, 0.30 mmol) was dissolved in ethanol (2 mL). Pivalic acid (138 μL, 1.20 mmol), sodium methoxide (81 mg, 1.50 mmol), and H_2ICIMP (68 mg, 0.15 mmol) were separately dissolved in ethanol (3 mL). The ligand solution was added to the zinc solution to give a faint yellow solution. The solution was heated to 50 °C and stirred. After 1 h the mixture had become slightly cloudy, and after the mixture was stirred overnight, a thick precipitate had formed. The white solid was filtered out, washed with ethanol, and dried to yield 54 mg (49%). FAB-MS [*m*/*z* (rel intensity, %)]: 1467 ([Zn_4(ICIMP)$_2$(Me_3Ac)$_2$$ClO_4$], 7), 683 ($Zn_2$(ICIMP)($Me_3$Ac), 100). IR (KBr disk; cm^{-1}): 3437 (w), 3124 (m), 2958 (s), 2925 (m), 2866 (m), 2362 (w), 2337 (w), 1605 (s), 1561 (s), 1515 (m), 1508 (m), 1480 (s), 1421 (s), 1375 (m), 1360 (m), 1335 (m), 1321 (w), 1303 (w), 1284 (m), 1163 (m), 1101 (s), 1077 (s), 953 (w), 928

(38) Bonfa, L.; Gatos, M.; Mancin, F.; Tecilla, P.; Tonellato, U. *Inorg. Chem.* **2003**, *42*, 7737.
(39) Mikkola, S.; Stenman, E.; Nurmi, K.; Yousefi-Salakdeh, E.; Strömberg, R.; Lönnberg, H. *J. Chem. Soc., Perkin Trans. 2* **1999**, 1619.

(w), 893 (w), 873 (w), 804 (w), 792 (w), 679 (w), 623 (m), 596 (w), 555 (w). UV/vis (MeCN; nm): 292 (s). NMR (MeCN-d_3): δ 1.22 (s), 1.28 (s), 2.14 (s), 3.26 (m), 3.36 (m), 3.55 (m), 3.81 (m), 3.86 (m), 3.90 (d), 6.59 (s), 6.75 (s), 6.84 (s), 6.96 (s), 6.92 (s). Anal. Calcd for $C_{58}H_{82}Cl_2N_{12}O_{18}Zn_4$: C, 44.43; H, 5.27; N, 10.72; Cl, 4.52. Found: C, 43.73; H, 5.18; N, 10.17; Cl, 4.94.

$[Zn_4(ICIMP)_2(Ph_2Ac)_2][ClO_4]_2$ (5). Zinc perchlorate hexahydrate (112 mg, 0.30 mmol) was dissolved in ethanol (2 mL). Diphenylacetic acid (254 mg, 1.20 mmol), sodium methoxide (81 mg, 1.50 mmol), and H_2ICIMP (68 mg, 0.15 mmol) were dissolved separately in ethanol (5 mL each) and mixed. The ligand solution was added to the zinc solution. The solution was heated to 60 °C and stirred. First a clear yellowish solution was obtained. After 5 min, a white precipitate was seen, which quickly grew thick. The mixture was stirred for 3 h, and then the precipitate was filtered out, washed, and dried to yield 82 mg (61%). Crystals of X-ray of quality could be grown by slow diffusion of *tert*-butyl methyl ether into a DMF solution of **5**. FAB-MS [*m*/*z* (rel intensity, %)]: 793 ([Zn_2(ICIMP)(Ph_2Ac)], 100). IR (KBr disk; cm^{-1}): 3437 (w), 3145 (w), 3121 (w), 3027 (w), 2973 (m), 2926 (m), 2860 (m), 2021 (w), 1607 (s), 1592 (s), 1546 (w), 1508 (m), 1477 (s), 1458 (m), 1398 (s), 1334 (m), 1307 (m), 1284 (w), 1264 (w), 1161 (m), 1096 (s, br), 958 (w), 744 (m), 698 (m), 647 (w), 623 (m), 501 (w). UV/vis (MeCN; nm): 292 (s). NMR (MeCN-d_3): δ 1.02 (s, br), 2.14 (s), 3.04 (m), 3.27 (m), 3.33 (m), 3.52 (m), 3.55 (m), 3.73 (m), 4.01 (d), 5.15 (s, br), 6.56 (s), 6.64 (s), 6.74 (s) 6.88 (s) 7.30 (s, 2H), 7.37 (s, 2H), 7.49 (s, 1H). Anal. Calcd for $C_{76}H_{86}Cl_2N_{12}O_{18}Zn_4$: C, 51.05; H, 4.85; N, 9.40; Cl, 3.97. Found: C, 51.04; H, 4.92; N, 8.77; Cl, 4.29.

X-ray Crystal Structure Determination. The crystal was immersed in cryo-oil, mounted in a Nylon loop, and measured at 150 K temperature. The X-ray diffraction data were collected with a Nonius KappaCCD diffractometer using Mo Kα radiation (λ = 0.710 73 Å). The Denzo-Scalepack[37] program was used for cell refinement and data reduction. The structure was solved by direct methods using the SHELXS-97[38] program with the WinGX[39] graphical user interface. An empirical absorption correction was applied to the data using XPREP in SHELXTL version 6.12[40] (T_{max}/T_{min}: 0.28035/0.24856). Structural refinement was carried out with SHELXL-97.[41] All hydrogens were placed in idealized positions and constrained to ride on their parent atom. The crystallographic data are summarized in Table 1.

Kinetic Measurements. The kinetic studies were performed in 3 mL UV cells in 1:1 H_2O−MeCN solution. The solution was buffered using Tris buffer (0.01 M total concentrated). The ionic strength was maintained at 0.1 by addition of sodium perchlorate (0.1 M). Dissolved complexes were added to a total concentration of 0.25 mM of dinuclear complex, and 2-hydroxypropyl *p*-nitrophenyl phosphate (HPNP, 0.82 mM) was used as substrate. All the ingredients were mixed, and the visual spectrum was recorded at 400 nm, where the extinction coefficient for the hydrolysis product *p*-nitrophenolate is 18 500 M^{-1} cm^{-1}. The data were plotted, and the linear slope was used to deduce the initial rates. The total amount of *p*-nitrophenol/phenolate was determined on the basis of its pK_a (7.15).[37]

DNA Hydrolysis Studies. Plasmid DNA (pUC18) was purchased from Sigma-Aldrich. To remove EDTA and buffer, the DNA was precipitated with ethanol and redissolved in water to an approximate concentration of 20 nM. DNA was incubated at different pH (HEPES at pH 7 and CHES at pH 10, 15 mM) and with and without catalyst. Electrophoresis was performed on a 1% agarose gel with ethidium bromide. TAE was used as buffer. The populations of the lanes are specified in the caption to Figure 5.

Acknowledgment. This research is supported by grants from the Swedish Research Council (VR, to E.N.) and the Academy of Finland (to M.H.). We thank Pal Papsai and Sofi Elmroth for their kind assistance in the preparations for the DNA experiments and Einar Nilsson for assistance in the recording of the high-resolution mass spectra.

Supporting Information Available: Crystallographic data in CIF format and a compiled list of NMR shifts (PDF). This material is available free of charge via the Internet at http://pubs.acs.org.

IC0354522